Origin of lipid tilt in flat monolayers and bilayers

Boris Kheyfets [*] and Sergei Mukhin

National University of Science and Technology MISIS, Leninskiy Prospekt, 4, Moscow 119049, Russia

Timur Galimzyanov

A.N. Frumkin Institute of Physical Chemistry and Electrochemistry RAS and National University of Science and Technology MISIS, Leninskiy Prospekt, 4, Moscow 119049, Russia

This paper continues the series of our works devoted to the liquid-gel phase transition in lipid membranes. Previously we described a variation of area per lipid, membrane thickness, and diffusion coefficient at the temperature-driven liquid-gel phase transition in bilayers. Here we expand the application of our analytic model approach to include a description of the lipid tilt and also extend the investigation to include Langmuir and self-assembled monolayers. The theory describes tilt formation at the temperature-driven liquid-gel phase transition in bilayers and the pressure-driven phase transition in Langmuir monolayers. Neither uniform tilt nor liquid-gel phase transition is found in self-assembled monolayers chemically bonded to the substrate.

I. INTRODUCTION

Twenty-five years have passed between the introduction of the fluid mosaic model [1] that considered the lipid bilayer of the cell membrane as merely holding the proteins and the discovery of the lipid-protein domains [2], indicating that lipids sometimes play a more active role in biochemical functions. It took even longer to realize the role played by lipid tilt (with respect to the membrane's normal) in the elastic energy of the lipid membrane, starting from the application of elasticity theory to the membranes [3] and generalizing the elastic energy functional to include the tilt deformation [4,5]. Currently, lipid tilt is recognized to play an important role for fusion [6,7], fission [8,9] of lipid bilayers, defines membrane dynamics at short wavelengths [10], and generally helps to relax the stress induced by membrane inclusion [11–14] and the domains boundary [15,16].

Physiologically relevant single-component liquid lipid bilayers usually exhibit no tilt in the ground state. The latter is observed experimentally for both lipid bilayers in gel phase [17] and lipid monolayers under lateral pressure in the Langmuir setup [18,19]. The physical origin of the uniform tilt in lipid membranes has been suggested several times in the literature [17,20–23]: the lipid glycerol group which links the hydrophilic head-group and hydrophobic tails limit the compression of lipids in a membrane. If the cross section of the lipid tails is smaller than the size of the glycerol "neck," tails can potentially lower the lipid free energy via the van der Waals attraction by tilting the tails together (see Fig. 1). For example, Dipalmitoylphosphatidylethanolamine phospholipid (DPPE) lipid differs from Dipalmitoylphosphatidylcholine phospholipid (DPPC) lipid only by a smaller head-group; however, there is no tilt at room temperature in bilayers composed of DPPE lipids [21], while bilayers composed of DPPC lipids do have a uniform tilt at room temperature, even though the temperature of transition to gel phase for a DPPE bilayer is higher compared to the transition to gel-phase temperature for a DPPC bilayer.

To the best of our knowledge, no attempt has been made to verify this explanation with molecular-level calculations, which could be useful for clarifying the details of the explanation of uniform tilt. The main subject of this paper is the calculation of the tilt in various single-component lipid membranes: bilayers, Langmuir monolayers, and monolayers chemically bonded to the substrate.

Throughout the paper, DPPC is used as a reference lipid, as it is the most characterized one. As there is no tilt in DPPC lipids in the liquid-disordered state [20], that is, at temperatures above 314 K, we start with a review of our previous derivation of liquid-gel phase transition [24], also called the main transition. For the convenience of the reader calculation of the liquid-gel phase transition is briefly reviewed below. This is followed by a calculation of the tilt angle for the lipid bilayer and monolayer, as well as the tilt angle of the monolayer with lipids chemically bonded to the substrate (see, e.g., [25,26]). Finally, we discuss calculation approaches that did not succeed and give arguments in favor of the approach used below in calculation of the tilt angle.

A. Flexible strings model

We treat the lipid membrane in the framework of the previously introduced flexible strings model [24,27–31], a mean-field theory that considers lipid in a self-consistent entropic repulsion field of other lipids in the same monolayer. Leaflets of a bilayer membrane are assumed to slide freely with respect to each other. Lipid in a single monolayer is modeled as an effective flexible string with a given incompressible area and finite bending rigidity (see Fig. 2), subjected to the
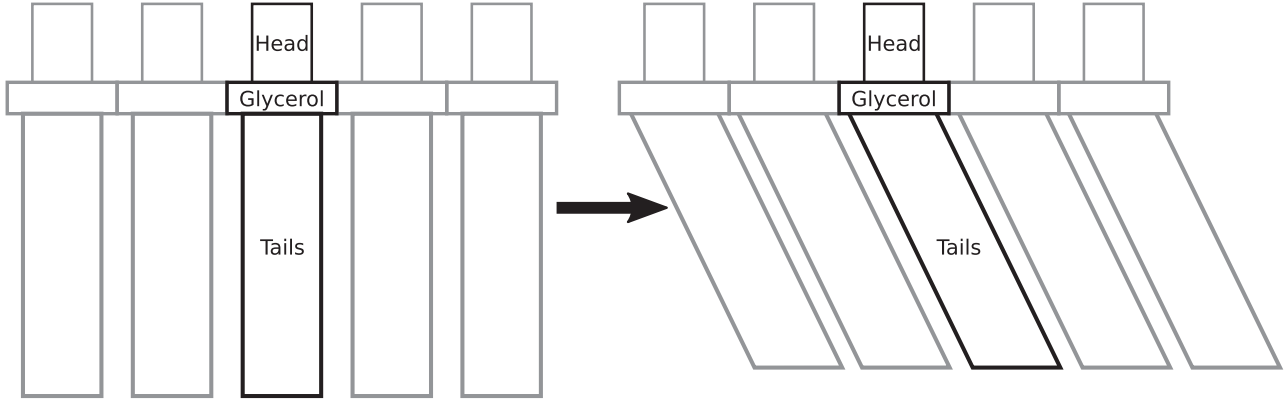
---
[*]kheyfboris@misis.ru

FIG. 1. Origin of the tilt. The lipid can lower its free energy by getting tails closer to each other, thereby increasing van der Waals attraction. However, if the area per tails is sufficiently small, due to the glycerol "neck" this is possible only by tilting the tails together.

self-consistent confining parabolic potential. The latter models a repulsive entropic force induced between the neighboring lipid molecules in the same monolayer due to the excluded volume effect (see Fig. 3). Interaction between head-groups is effectively included in surface tension in the hydrophobic region. The energy functional of the string consists of kinetic energy and bending energy of a given dynamical string conformation, as well as potential energy in the confining potential induced by collisions with the neighboring strings:

$$E_t = \int_0^L \left[\frac{\rho \dot{\mathbf{R}}^2}{2} + \frac{K_f}{2} \left(\frac{\partial^2 \mathbf{R}}{\partial z^2} \right)^2 + \frac{B\mathbf{R}^2}{2} \right] dz \,, \qquad (1)$$

where ρ is a string linear density, $\mathbf{R}(z) = \{R_x(z), R_y(z)\}$ is a vector in the plane of the membrane, giving deviation of

a string from the straight line as a function of coordinate z along the axis normal to the membrane plane (see Fig. 2), and B is a parameter of the confining potential determined self-consistently. The self-consistent parabolic potential has been used previously to model a polymer chain in confined geometry [32]. That approach is conceptually close to the statistical kink model [33,34], which was used to find the probability distribution function of chain conformations and macroscopic membrane characteristics by minimizing the free energy of the membrane. In contrast to that model, we use the continuous description of the bending fluctuations of a lipid chain and include an option of the direct self-assembly of lipids in a membrane.

Boundary conditions for a model flexible string take into account the following physical assumptions [the same is assumed also for component $R_y(z)$]:

$R_x'(0) = 0$ a chain terminates perpendicularly to the membrane surface

$R_x'''(0) = 0$ net force acting on a head is zero

$R_x''(L) = 0$ net torque acting at a chain's free end is zero

$R_x'''(L) = 0$ net force acting at a chain free end is zero   (2)

The first boundary condition reflects the orientational asymmetry of the monolayer due to the water-lipid interface, which is clearly seen from data on the molecules orientational order parameter [35,36]: lipid tails are more ordered in the vicinity of head-groups constrained by the hydrophobic tension. Yet, the chains are not permanently perpendicular to the membrane surface, and boundary conditions are approximate and necessary to keep the model analytically solvable. The other boundary conditions reflect the freely moving lipid head-group and hydrocarbon tail end: zero force acting on the head-group and zero momentum and force acting on the lipid tail end.

Assuming membrane to be locally isotropic in the lateral plane, we split partition function into a product of two equal components, $Z = Z_x Z_y = Z_x^2$, and thus the free energy of the lateral oscillations of the chain equals

$$F_t = -2k_B T \log Z_x \,. \qquad (3)$$

The partition function Z_x could be written as a path integral over all chain conformations:

$$Z_x = \iint e^{-\frac{E\{R_x(z), \dot{R}_x(z)\}}{k_B T}} DR_x D\dot{R}_x. \qquad (4)$$

Under the boundary conditions Eq. (2), the potential energy part of the functional Eq. (1) can be equivalently rewritten in terms of the linear Hermitian operator $\hat{H} = B + K_f \frac{\partial}{\partial z^4}$ in the form

$$E_{t(\text{pot})} = \sum_{\alpha = x, y} E_\alpha E_\alpha \equiv \int_0^L [R_\alpha(z)\hat{H}R_\alpha(z)] \, dz. \qquad (5)$$

Then an arbitrary conformation of the chain is expressed as the deviation of the centers of the string $R_{x,y}(z)$ from the straight vertical line (see Fig. 2) and is parameterized by an infinite set of coefficients C_n of the linear decomposition of the function $R_{x,y}(z)$ over the eigenfunctions $R_n(z)$ of the
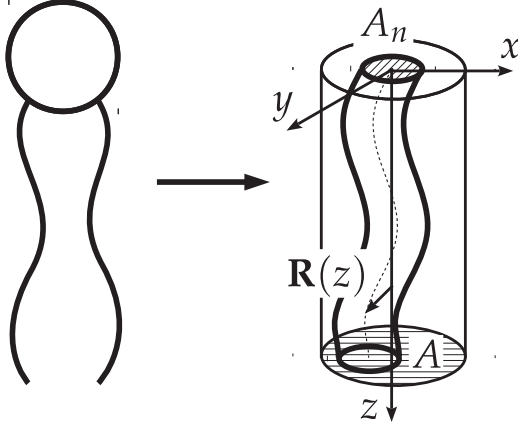
FIG. 2. Hydrocarbon tails of the lipid molecule are modeled as a flexible string. Schematic representation.

operator $\hat{H}$:

$$R_{\alpha=x,y}(z) = \sum_n C_{n,\alpha} R_n(z), \quad \hat{H} R_n(z) = E_n R_n(z). \quad (6)$$

Substituting Eq. (6) into Eq. (1) and using the standard orthogonality property of the eigenfunctions of operator $\hat{H}$ enables a simple decomposition of the energy functional into the series

$$E_t = \sum_n \frac{1}{2} \{ \rho \dot{C}_n^2 + E_n C_n^2 \}. \quad (7)$$

We thus see that energy of a fluctuating string in parabolic potential maps on the sum of energies of harmonic oscillators with rigidities E_n. Hence, the Boltzmann's probability of the state of a string in an arbitrary conformation $R_{x,y}(z)$, $P(\{R_{x,y}(z)\})$, is proportional to the infinite product of the Boltzmann probabilities of the states of these oscillators due to the following obvious relation:

$$P(\{R_{x,y}(z)\}) \propto \exp\left\{-\frac{E_t}{k_B T}\right\} \sim \prod_n \exp\left\{-\frac{\varepsilon_n}{k_B T}\right\}$$

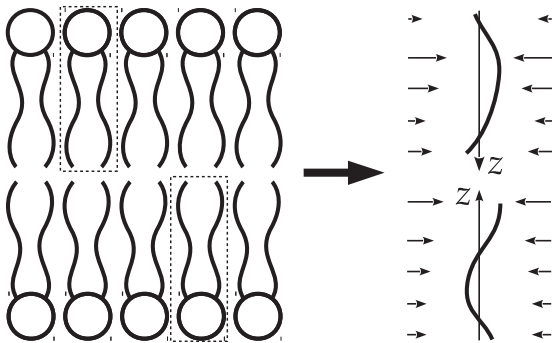$$\varepsilon_n \equiv \frac{1}{2}\{\rho \dot{C}_n^2 + E_n C_n^2\}. \quad (8)$$

FIG. 3. Collisions with neighboring lipids are modeled by self-consistent confining potential. Potential is a parabolic function of the string deviation amplitude from axis z (arrow sizes mimic local force strength).

Therefore distribution of the coefficients C_n proves to be just a Gaussian Boltzmann distribution, which makes the whole thermodynamic theory of the lipid membrane analytically tractable. The corresponding eigenvalues E_n and eigenfunctions $R_n(z)$ of the operator $\hat{H} = B + K_f \frac{\partial^4}{\partial z^4}$ are [27]

$$n = 0 \Rightarrow \begin{cases} E_0 = B \\ R_0(z) = \sqrt{\frac{1}{L}} \end{cases}$$

$$n \in \mathbb{N} \Rightarrow \begin{cases} c_n = \pi n - \frac{\pi}{4} \\ E_n = B + c_n^4 \frac{K_f}{L^4} \\ R_n(z) = \sqrt{\frac{2}{L}} \left[\cos\left(c_n \frac{z}{L}\right) + \frac{\cos(c_n)}{\cosh(c_n)} \cosh\left(c_n \frac{z}{L}\right) \right]. \end{cases}$$
$$(9)$$

This gives the following product of the Gaussian integrals for the partition function:

$$Z_x = \int_{-\infty}^{+\infty} \prod_n e^{-\frac{(\rho \dot{C}_n)^2}{2\rho k_B T} - \frac{C_n^2 E_n}{2k_B T}} \frac{d(\rho \dot{C}_n) dC_n}{2\pi \hbar} = \prod_n \frac{k_B T}{\hbar} \sqrt{\frac{\rho}{E_n}}. \quad (10)$$

To derive the dependence of the monolayer thickness on the temperature we relate it to the contour length of the lipid chain L_R proportional to the number of CH_2 groups in the lipid tail:

$$L_R = \int_0^L \sqrt{1 + \left\langle \left(\frac{\partial \vec{R}}{\partial z}\right)^2 \right\rangle} \, dz. \quad (11)$$

Expanding this finally yields an equation which might be solved numerically:

$$L_R = L + \frac{2k_B T L^2}{K_f} \sum_{n=1} \frac{c_n^2 \int_0^1 \left(\sin(c_n x) - \frac{\cos c_n}{\cosh c_n} \sinh(c_n x)\right)^2 dx}{B + c_n^4 \frac{K_f}{L^4}} \quad (12)$$

(for derivation see Appendix A in [31]).

To derive the self-consistency equation for the so far unknown parameter B, we differentiate both sides of Eq. (3) with respect to B and readily obtain the self-consistency equation for this parameter:

$$\frac{\partial F_t}{\partial B} = L \langle R_x^2 \rangle, \quad (13)$$

where brackets denote the thermodynamic (Boltzmann) average over chain conformations. The right-hand side of Eq. (13) is directly expressed via the thermodynamic average area per lipid A in the membrane plane and effective incompressible area of lipid chain A_n:

$$\pi \langle R_x^2 + R_y^2 \rangle = 2\pi \langle R_x^2 \rangle = (\sqrt{A} - \sqrt{A_n})^2, \quad (14)$$

where we utilized the isotropy of the membrane in the plane. Using this relation and exploiting Eq. (10), one can rewrite Eq. (13) in the explicit form

$$\sum_{n=0} \frac{1}{B \frac{L^4}{K_f} + c_n^4} = \frac{K_f A_n}{\pi k_B T L^3} \left(\sqrt{\frac{A}{A_n}} - 1\right)^2. \quad (15)$$

This is the self-consistency equation, as it links parameter of the mean field B with the mean area per lipid A.

We also compute the orientational chain order parameter [37] for a given hydrocarbon position, z: $S_z(z) = \frac{1}{2}(3\langle\cos^2\theta(z)\rangle - 1)$. One can replace the mean cosine with a tangent via $\langle\cos^2\theta(z)\rangle = 1/(1 + \langle\tan^2\theta(z)\rangle)$. Finally, a mean local tangent can be expressed via expansion over eigenfunctions:

$$\langle\tan^2\theta(z)\rangle$$
$$= \langle(\vec{R}'(z))^2\rangle = 2\sum_{n=0}\langle C_n^2\rangle(R_n'(z))^2 = 2k_BT\sum_{n=0}\frac{(R_n'(z))^2}{E_n}. \quad (16)$$

The average over the hydrocarbon group position order parameter is sometimes used to compare the overall order of the lipid chain [38]. This parameter is useful for analysis of the system behavior in the absence of a phase transition.

B. Liquid-gel phase transition in lipid bilayers

The total free energy of the lipid monolayer consists of entropic repulsion, Eq. (9), hydrophobic tension, and van der Waals attraction between the lipid tails:

$$\frac{F_T}{k_BT} = \frac{F_t(A)}{k_BT} + \frac{\gamma A}{k_BT} - \frac{9\pi^{7/2}}{2^8}\frac{UN^2}{LA^{5/2}k_BT}. \quad (17)$$

Here γ is the hydrophobic tension and U is the van der Waals parameter.

The nature of hydrophobic tension consists of a number of interactions and cannot be reduced to the contact of water molecules with the hydrophobic chain. These interactions include attraction of hydrophilic heads to water, repulsion of hydrophobic tails from water, steric interactions between lipid heads, the contribution of the hydration force, and an electrostatic double-layer contribution if the head-groups are charged [39]. A full account of all these contributions will make the model intractable, complex, and it will bring a number of poorly known parameters, which will not contribute to the clarity of the description of the tilt phase. A common and very effective approximation is a reduction of all the aforementioned interactions via casting them together into single effective surface energy proportional to the area of the lipid-water interface. However, as we discriminate between area per lipid at the lipid-water interface and cross-section area per hydrocarbon tail, only the latter appears to be applicable. Attributing the interface area to the head-group interface leads to an unphysically large drop of the total driving force at the point where the area reaches the head-group area, $A = A_h$, and results in the absence of tilt in the gel phase of the DPPC lipids.

Another approach to calculate the system's free energy was used in Ref. [40], in which the following lipid energy contributions were considered: the internal energy related to a number of trans and gauche orientations in a particular lipid conformation, dispersive energy related to van der Waals interaction with neighboring lipids, and steric repulsion taken in the linear approximation. The total lipid energy was then used to compute partition function and free energy of the
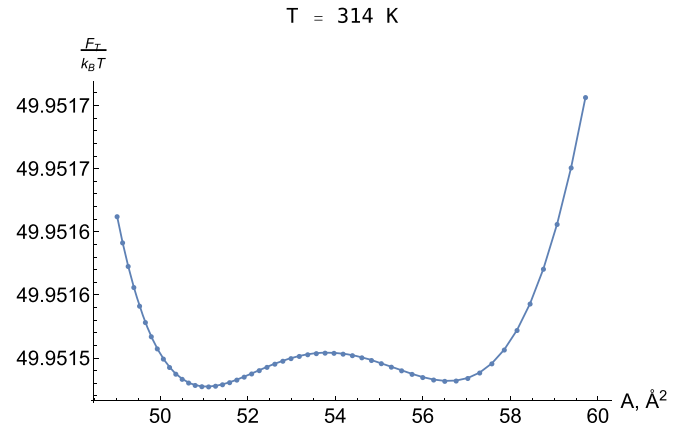

FIG. 4. Main phase transition in DPPC bilayer.

system. By contrast, in our model steric repulsion is computed self-consistently via Eq. (15), whereas van der Waals interaction and hydrophobic tension are included directly into the free energy of the chain, via Eq. (17). Our approach allows us to discriminate between cross-section area per hydrophobic chain and water-membrane surface area per lipid—the distinction which we found important for the origin of the tilt, which seems to be problematic to explain within the approach of [40].

After renormalization of Eq. (17) by the energy of the rigid rod subject to the boundary conditions of Eq. (2) (the result is Eq. (12) of [24], and reference to the derivation is also found there), the three contributions of Eq. (17) provide the double-minima dependence of the free energy on area A, describing a first-order liquid-gel phase transition. Equilibrium area per lipid is found by minimizing free energy Eq. (17) with respect to the area per lipid. The main phase transition is characterized by two minima (see Fig. 4). The liquid-gel phase transition is also prominent with regard to the mean order parameter [see text after Eq. (16)] dependence on the temperature (see Fig. 5).

C. Tilt in lipid membranes

A nonzero lipid tilt angle α enables the lipid tails approximation, thus making the area per tail A smaller than the area
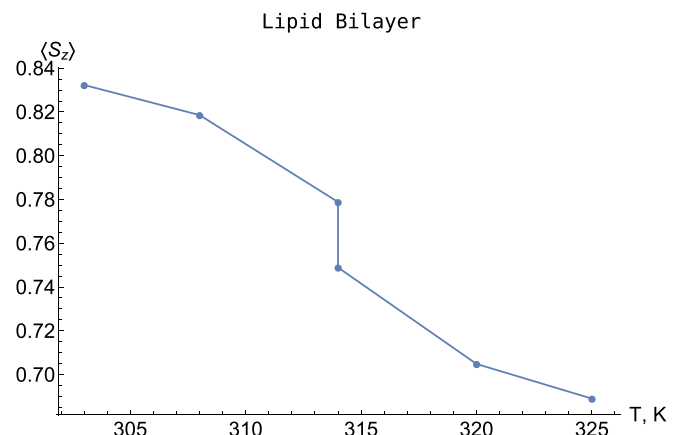

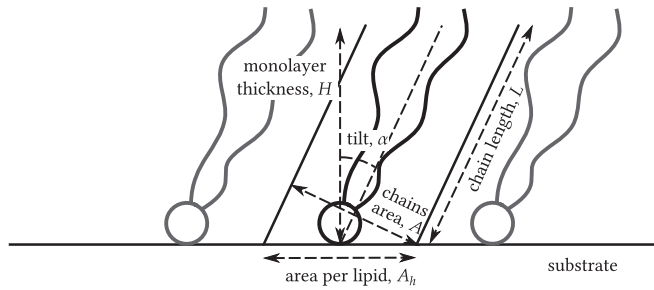FIG. 5. DPPC bilayer mean order parameter dependence on the temperature.

FIG. 6. Lipid monolayer with a tilt.

per head A_h, and the lipid length L larger than the membrane thickness H. The relations are straightforward [17]:

$$H = L_R \cos \alpha$$
$$A_h = \frac{A}{\cos \alpha} \quad (18)$$

(see Fig. 6).

II. TILT IN LIPID MEMBRANES

A. Tilt in lipid bilayers

In the first approximation, area per lipid in the gel phase does not depend on the temperature [17], since lipid tails condense by increasing the tilt angle. Treating cross-section area per tail as the area featured in the total lipid free energy, Eq. (17), allows us to compute the tilt angle using Eq. (18). Calculated tilt angle dependence on the temperature is plotted in Fig. 7 (solid line with triangles). We use the following parameter values for calculation: 21 Å^2 for incompressible area A; 47.3 Å^2 for lipid head area A_h [17]; 16 Å for total chain length L_R; 4.28×10^{-21} erg cm for effective chain bending modulus K_f; 798.4 kcal Å^6/mol for van der Waals parameter U [41]; and 19.5 erg/cm^2 for hydrophobic tension γ [39].

As the temperature drops below 314 K, DPPC lipids undergo a transition to the gel phase. At about 313 K the surface
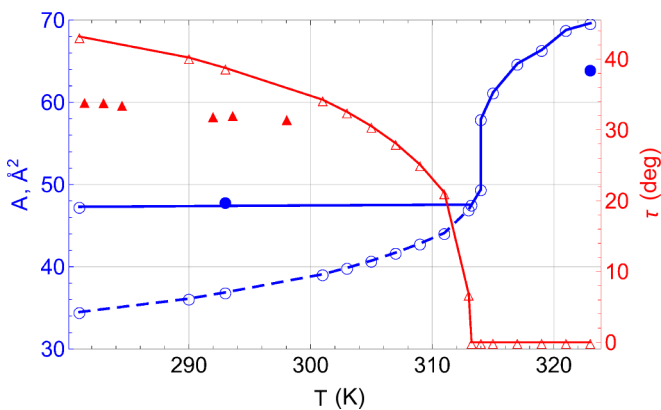

FIG. 7. Solid line with empty triangles shows computed tilt angle for DPPC bilayer. Filled triangles show measured DPPC bilayer tilt angle values [17]. Line with empty circles shows calculated cross-section area of DPPC tails. Area per lipid is defined by the lipid tails as long as cross-section area per tail exceeds the area per lipid head. Filled circles show experimental data for area per lipid in DPPC [17].
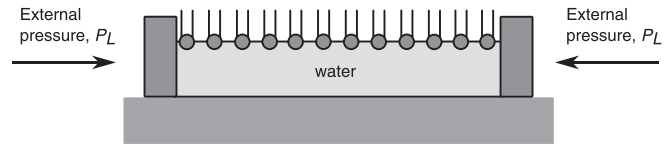

FIG. 8. Langmuir monolayer setup. Area per lipid is set by the external pressure applied to barriers.

area of the lipids is effectively locked by the glycerol "necks." However, due to the tilt angle increase, the cross-section area per lipid tail continues to decrease with lowering the temperature (Fig. 7, dashed line). The difference between the cross-section area per lipid tail and area per lipid head leads to a tilt of the lipid tails (Fig. 7, solid line with triangles). Filled triangles and circles show the experimental data for DPPC tilt and area per lipid (both taken from [17]).

A fully saturated DPPC bilayer does not have a well-defined gel phase transition temperature: at 314.3 K, part of the lipids start to condense into gel phase, with all of the bilayer becoming a gel phase only below 308.4 K. In between these temperatures, liquid and gel phases coexist in the membrane, which results in a so-called ripple phase [42–44]. However, the temperature region (308.4–314.3 K) in Fig. 7 implies the existence of the gel phase alone. This discrepancy is due to the limitation of our model, which is a first-order phase transition model and thus does not account for the transitive states and allows only one phase in the finite temperature region.

B. Tilt in Langmuir monolayers

A Langmuir monolayer is lipid monolayer formed in a water bath. The setup allows for an easy change of the bath area with the help of the mobile barriers (see Fig. 8), and thus allows changing the area per lipid at a fixed temperature. A typical pressure-area isotherm of the lipid monolayer in the Langmuir setup includes a gaslike phase at low pressures, with a liquid-disordered phase formed with increasing the pressure, and finally, a transition to a gel phase at high pressures [18,19,45].

Treating the external pressure P_L as the hydrophobic tension γ featured in Eq. (17) allows us to reproduce a pressure-driven liquid-gel phase transition in the Langmuir setup (see Fig. 9).

In contrast to a lipid bilayer, it is possible to compress Langmuir monolayer lipids slightly tighter than the lipid head's area (marked with the filled square in Fig. 9). A decrease of tilt has been reported for Dimyristoylphosphatidyl-choline phospholipid (DMPC) Langmuir monolayers for pressures above the phase transition point (see Fig. 3 and Table 1 in Ref. [45]). In our approach, we neglect the compressibility of the lipid heads, compared to the compressibility of lipid chains. As seen from Fig. 9, this assumption does not hold in the pressure-induced gel phase of the Langmuir monolayer. However, as our calculation of area per tails still holds (dashed line in Fig. 9), a tilted to nontilted transition in Langmuir monolayers at high pressure, reported, e.g., for DMPC in [45], can be explained by decreasing the tilt-related free energy benefit caused by taking the proper account of compressibility of the lipid heads. For example, Fig. 10 depicts the calculated
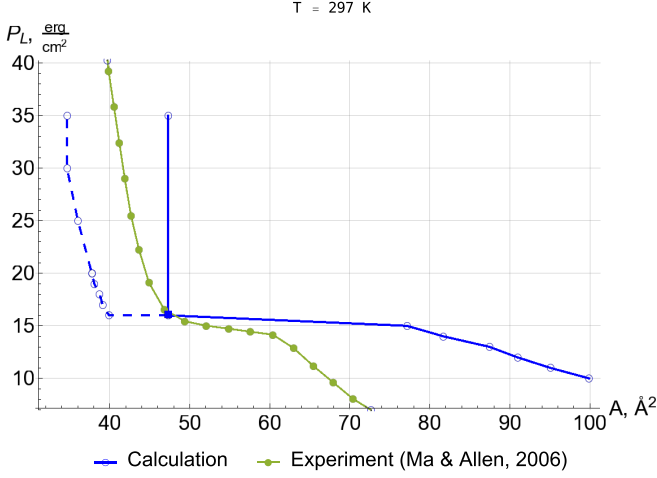
FIG. 9. Liquid-to-gel pressure-driven DPPC phase transition at 297 K (Langmuir setup, see Fig. 8). Equation of state is the same as for a bilayer, Eq. (17), with external pressure (see Fig. 8) P_L taking part of hydrophobic tension γ. Dashed line shows area per tails in the gel phase.

free energy of hydrocarbon tails of the DPPC Langmuir monolayer at 297 K and external pressure of 18 dyn/cm. The experimental area per lipid under this condition is about 46 Å^2 (see Fig. 9). As the optimal area per tails is lower than that (free energy minimum is at 38 Å^2), the Langmuir monolayer under pressure of 18 dyn/cm is tilted. A vanishing tilt at higher pressure, which is observed, e.g., for DMPC [45], could be explained by heads compression at higher pressure, thus fitting to the area per tails.

Finally, we computed the transition pressure dependence on temperature for the DPPC Langmuir monolayer (see Fig. 11). It matches our expectation of higher temperature requiring higher pressure at the phase transition.

C. Bonded lipid monolayers

Another system we have considered in this work is the self-assembled monolayers chemically bonded to the substrate,
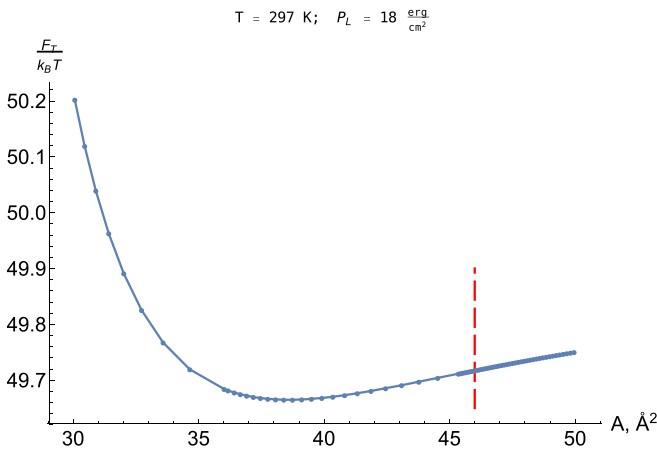

FIG. 10. Calculated free energy of hydrocarbon tails of DPPC Langmuir monolayer at 297 K and external pressure of 18 dyn/cm. Experimental area per lipid under these conditions is about 46 Å^2 (shown here with dashed line, also see Fig. 9).
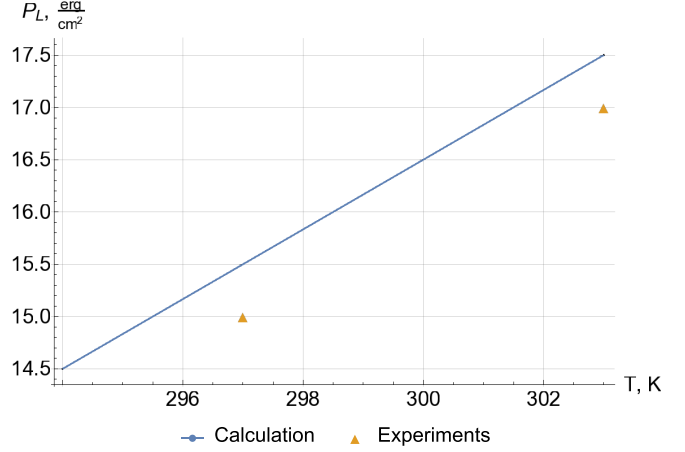

FIG. 11. Pressure-driven liquid-to-gel phase transition pressure dependence on temperature for DPPC. Experimental data from [18,19].

which models various types of surface coverings (for a review see, e.g., [26]). An abstract common picture is the following: a rigid link fixes the head-group coordinate, however, allowing the hydrocarbon chain inclinations, thus imposing the following boundary conditions at the lipid chain head: $R(0) = 0$ and $R''(0) = 0$, instead of $R'(0) = 0$ and $R'''(0) = 0$. These equations, together with the two conditions at the lipid chain end: $R''(L) = 0$ and $R'''(L) = 0$ [see Eq. (2)], are analytically solvable via the framework described in Sec. I A. Namely, the boundary conditions of the bonded lipid,

$R_x(0) = 0$ lipid head is bonded to the substrate

$R_x''(0) = 0$ the net torque acting on a chain's head is zero

$R_x''(L) = 0$ the net torque acting at a chain's free end is zero

$R_x'''(L) = 0$ the net force acting at a chain's free end is zero, (19)

allows one to rewrite the energy functional Eq. (1) in operator form, with the same operator $\hat{H} = B + K_f \frac{\partial^4}{\partial z^4}$. Orthonormalized eigenvalues and eigenfunctions of the operator subject to the boundary conditions Eq. (19) are

$$c_n = \pi n + \frac{\pi}{4}, \quad n \geqslant 1$$

$$R_n = \frac{\sqrt{2}}{L}\left[\sin(c_n z) + \frac{\sin c_n}{\sinh c_n}\sinh(c_n z)\right] \quad (20)$$

$$E_n = B + c_n \frac{K_f}{L^4},$$

which is analogous to Eq. (9) for nonbonded lipids.

Eigenfunctions of the bonded lipid, Eq. (20), result in a different expression for the steric repulsion energy, which is featured in the free energy Eq. (17). The free energy Eq. (17) has to be renormalized by that of a rigid rod with the boundary conditions of a bonded lipid, Eq. (19) (see Appendix A for the derivation). Our calculation of the bonded DPPC monolayer yields a monotonously decreasing free energy, with the maximum cross-section area A (see Fig. 6) of the free lipid ($B = 0$) being $A_{max} \approx 40$ Å^2 (see Fig. 12).
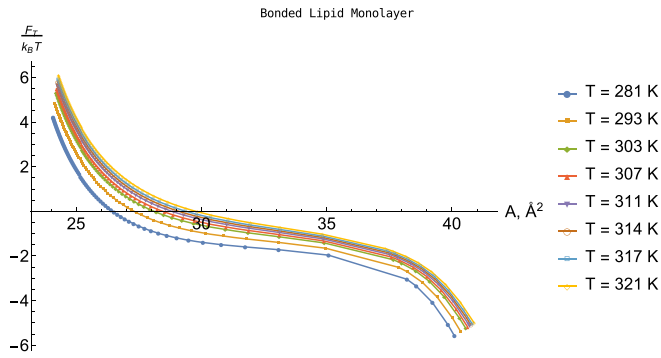
FIG. 12. Neither uniform tilt, nor temperature- or pressure-driven liquid-gel phase transition are found for a lipid monolayer chemically bonded to a substrate.

If we bind lipids to the substrate, so that the area per lipid is greater than A_{max}, it follows then that lipids do not "feel" each other, since in that region the mean-field steric repulsion parameter is zero, $B = 0$. Hence, the tilt in that region is also zero: lipids simply do not interact sterically and the shrinking distance between them does not change the free energy; therefore, a tilt would not yield the free energy decrease.

If, on the other hand, we bind lipids to the substrate so that area per lipid is smaller than A_{max}: $A_{bind} < A_{max}$, it means that the tilt is only possible if there would be a smaller free energy at some smaller area. This condition proves to be unfulfilled, as calculated free energy is found to be a monotonous function of the area per lipid tail. Hence we conclude, that for bonded lipids a phase with uniform tilt is less favorable compared to a nontilted phase.

III. DISCUSSION

We examined a conjecture that the difference between an area per lipid's tail and area per lipid's head is the smoking gun of lipid tilt in the lipid membranes. We demonstrated, using a simple microscopic model, that the above conjecture comes into play when hydrophobic tension is acting in the cross section of the lipid chains rather than being concentrated merely at the lipid heads. Besides that, we have shown that tilt emerges at both the temperature-driven liquid-gel phase transition in lipid bilayers (Fig. 7) and the pressure-driven liquid-gel phase transition in Langmuir monolayers. Finally, we found that our theoretical model does not predict any uniform tilt in lipid monolayers chemically bonded to a substrate.

Importantly, we found that the transition between tilted and nontilted states is not a direct consequence of the liquid-gel phase transition. This fact is eminent from our calculation, Fig. 7, where the transition to the gel phase precedes by 1 K a transition into a tilted state. Our calculation of area per tail via Eq. (17) implies that hydrophobic energy, γA, features area per tail rather than area per head. We explain it by noting that the physical origin of the hydrophobic energy is the contact of water molecules with the chains, and thus it is the cross-section area per tail that hydrophobic energy should depend on rather than the area per lipid head.

Attributing the interface area to the head-group interface leads to the unphysically large generalized force drop at the point $A = A_h$, where the $A < A_h$ energy term γA is replaced by a constant γA_h that does not contribute to the first derivative, thus leading to a drop of the generalized force $\partial F / \partial A$ by the value γ. The latter value is comparable to all other contributions, which leads to a very sharp free energy minimum at A_h and leads to a zero tilt for DPPC at room temperature, contrary to experiment. Another approach might be to change the boundary conditions, e.g., assuming that the lipid head position at the membrane surface $R(0)$ and torque applied to the lipid head $R''(0)$ are fixed in the gel phase. This approach leads to a drastic break in the slope of the free energy of the membrane as a function of area, which we think is unphysical.

Though we considered only homogeneous bulk phases, accounting for the dynamics of the phase transition and collective phenomena can indicate the emergence of multiple domains with different tilt directions and amplitudes, as it is described in the work of Ref. [46]. The full account of the phase transition details as well as a local-curvature-induced tilt phase [11,12] requires separate investigation and lies outside the scope of this paper.

Upon comparing scales of $F_T / k_B T$ values of bonded lipids (Fig. 12) with nonbonded lipids (Fig. 4) we see a difference of absolute values of free energies by an order of magnitude. This difference is caused by the different renormalization of bonded and nonbonded lipids. For this reason a direct comparison of absolute values of calculated free energies between the bonded and nonbonded is not meaningful. Instead, we compare a rate of decrease of computed values of total free energies with area and conclude that bonding leads to the higher decrease rate of the steric repulsion with lipid cross-section area, as two other contributions to the total free energy, namely, hydrophobic energy and van der Waals interaction, are the same for both bonded and nonbonded lipids.

This higher decrease rate of the steric repulsion energy with area in the case of bonded lipids can be understood as the effect that lipid head bonding exerts on the steric repulsion: the bond prevents lateral movement of the lipid molecules and thus causes reduction of the configurational volume available to each lipid, yielding, in turn, a faster decrease of the excluded volume effect with an increase of area per lipid compared to the nonbonded case. As a result, the change of steric repulsion dominates the total free energy change of the bonded lipids with area per lipid, making it monotonous, and hence makes either a liquid-gel phase transition or uniform tilt unfavorable, as explained in Sec. II C.

In summary, we have demonstrated that as the temperature lowers, entropic repulsion between lipids diminishes, and thus at some point van der Waals attraction between lipid tails becomes a viable source of decreasing lipid free energy. If the lipid heads are large enough to prevent lipid tails from approaching each other, then lowering of the lipid free energy occurs via a tilt of the lipid tails, which makes tails closer to each other relative to the state in which their axes are parallel to the normal to the membrane's surface. In the case of Langmuir monolayers, one can compress lipid-head regions to some extent by the external pressure to reach the point when the tilted state is no longer energetically advantageous. Thus, in the Langmuir monolayers tilt disappears at higher

pressures. Chemically bonded lipid monolayers are shown to have no uniform tilt. Modeling the lipid membrane energy functional with a mean-field self-consistent entropic repulsive potential, together with hydrophobic tension and van der Waals attraction between lipid tails, reproduces the liquid-gel phase temperature-driven transition in the bilayer as well as the pressure-driven transition in Langmuir monolayers, with a correct variation of area per lipid, tilt angle, and membrane thickness.

ACKNOWLEDGMENTS

APPENDIX: RENORMALIZATION OF BONDED CHAIN'S STERIC REPULSION ENERGY

Arbitrary bonded chain conformation and its energy might be expanded in eigenfunctions and eigenvalues [see Eq. (20)]:

$$R = \sum_{n=1} R_n C_n, \quad E_t = \sum_{n=1} E_n C_n, \quad \text{(A1)}$$

where C_n are time-dependant coefficients.

The free energy of bonded flexible string oscillations F_t diverges:

$$Z_x = \prod_{n=1} \frac{k_B T}{\hbar \omega_n} \Rightarrow F_t = 2k_B T \sum_{n=1} \log\left(\frac{\hbar \omega_n}{k_B T}\right) = \infty, \quad \text{(A2)}$$

where $\omega_n = \sqrt{E_n/\rho}$, ρ is a linear density of the string. One might renormalize F_t by the free energy of the rigid bonded string ($K_f \to \infty$) subject to the same boundary conditions of Eq. (19). For this, consider a nontrivial Jacobian involved in partition function calculation:

$$Z_x = \frac{1}{C} \prod_{n=1} \frac{k_B T}{\hbar \omega_n} \Rightarrow F_t = 2k_B T \sum_{n=1} \log\left(\frac{\hbar \omega_n}{k_B T}\right) + 2k_B T \log C. \quad \text{(A3)}$$
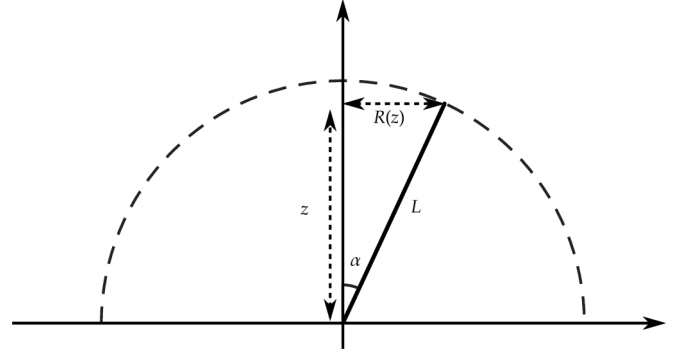

FIG. 13. The only displacement type of the bonded rigid rod.

The free energy equation (A3) can then be rewritten in the following form:

$$F_t = 2k_B T \log C + k_B T \sum_{n=1} \log \frac{\hbar^2}{(k_B T)^2 \rho} \frac{K_f}{L^4} c_n^4$$

$$+ k_B T \sum_{n=1} \log\left[1 + \frac{BL^4}{c_n^4 K_f}\right]. \quad \text{(A4)}$$

Considering rigid rod, $K_f \to \infty$, we can obtain its free energy as a limiting case of Eq. (A4):

$$F_t^{\text{rigid}} = 2k_B T \log C + k_B T \sum_{n=1} \log \frac{\hbar^2}{(k_B T)^2 \rho} \frac{K_f}{L^4} c_n^4. \quad \text{(A5)}$$

On the other hand, a bonded rigid rod has a single oscillation mode (see Fig. 13) and its partition function is known exactly:

$$Z_x = \int_{-\frac{\pi}{2}}^{\frac{\pi}{2}} e^{-\int_0^{L\cos\alpha} \frac{B}{2k_B T} z^2 \tan^2\alpha \, dz} \, d\alpha = \int_{-\frac{\pi}{2}}^{\frac{\pi}{2}} e^{-\frac{L^3}{3} \frac{B}{2k_B T} \cos\alpha \sin^2\alpha} \, d\alpha. \quad \text{(A6)}$$

Hence

$$F_t^{\text{rigid}} = -2k_B T \log \int_{-\frac{\pi}{2}}^{\frac{\pi}{2}} e^{-\frac{L^3}{3} \frac{B}{2k_B T} \cos\alpha \sin^2\alpha} \, d\alpha. \quad \text{(A7)}$$

Using Eqs. (A5) and (A8), one arrives at the free energy renormalized by subtraction from Eq. (A4) of the formally divergent expression Eq. (A5) and then compensating that subtraction by an equivalent (convergent) expression of the free energy of the bonded rigid rod in the form of Eq. (A8):

$$\frac{\tilde{F}_t}{k_B T} = \sum_{n=1} \log\left[1 + \frac{BL^4}{c_n^4 K_f}\right]$$

$$- 2\log\left[\int_{-\frac{\pi}{2}}^{\frac{\pi}{2}} e^{-\frac{L^3}{3} \frac{B}{2k_B T} \cos\alpha \sin^2\alpha} \, d\alpha\right]. \quad \text{(A8)}$$

[1] S. J. Singer and G. L. Nicolson, The fluid mosaic model of the structure of cell membranes, Science **175**, 720 (1972).

[2] K. Simons and E. Ikonen, Functional rafts in cell membranes, Nature (London) **387**, 569 (1997).

[3] W. Helfrich, Elastic properties of lipid bilayers: Theory and possible experiments, Z. Naturforsch, C: J. Biosci. **28**, 693 (1973).

[4] M. Hamm and M. M. Kozlov, Elastic energy of tilt and bending of fluid membranes, Eur. Phys. J. E **3**, 323 (2000).

[5] T. R. Galimzyanov, P. I. Kuzmin, P. Pohl, and S. A. Akimov, Elastic deformations of bolalipid membranes, Soft Matter **12**, 2357 (2016).

[6] S. A. Akimov, R. J. Molotkovsky, T. R. Galimzyanov, A. V. Radaev, L. A. Shilova, P. I. Kuzmin, O. V. Batishchev, G. F. Voronina, and Y. A. Chizmadzhev, Model of membrane fusion: Continuous transition to fusion pore with regard of hydrophobic and hydration interactions, Biochem. (Moscow) Suppl. Ser. A: Membr. Cell Biol. **8**, 153 (2014).

[7] R. Molotkovsky, T. Galimzyanov, I. Jiménez-Munguía, K. Pavlov, O. Batishchev, and S. Akimov, Switching between successful and dead-end intermediates in membrane fusion, Int. J. Mol. Sci. **18**, 2598 (2017).

[8] V. A. Frolov, A. Escalada, S. A. Akimov, and A. V. Shnyrova, Geometry of membrane fission, Chem. Phys. Lipids **185**, 129 (2015).

[9] V. A. Frolov, P. V. Bashkirov, S. A. Akimov, and J. Zimmerberg, Membrane curvature and fission by dynamin: Mechanics, dynamics and partners, Biophys. J. **98**, 2a (2010).

[10] E. R. May, A. Narang, and D. I. Kopelevich, Role of molecular tilt in thermal fluctuations of lipid membranes, Phys. Rev. E **76**, 021913 (2007).

[11] M. Fošnarič, A. Iglič, and S. May, Influence of rigid inclusions on the bending elasticity of a lipid membrane, Phys. Rev. E **74**, 051503 (2006).

[12] V. Kralj-Iglič, B. Babnik, D. R. Gauger, S. May, and A. Iglič, Quadrupolar ordering of phospholipid molecules in narrow necks of phospholipid vesicles, J. Stat. Phys. **125**, 727 (2006).

[13] S. A. Akimov, V. V. Aleksandrova, T. R. Galimzyanov, P. V. Bashkirov, and O. V. Batishchev, Interaction of amphipathic peptides mediated by elastic membrane deformations, Biochem. (Moscow) Suppl. Ser. A: Membr. Cell Biol. **11**, 206 (2017).

[14] O. V. Kondrashov, T. R. Galimzyanov, I. Jiménez-Munguía, O. V. Batishchev, and S. A. Akimov, Membrane-mediated interaction of amphipathic peptides can be described by a one-dimensional approach, Phys. Rev. E **99**, 022401 (2019).

[15] T. R. Galimzyanov, A. S. Lyushnyak, V. V. Aleksandrova, L. A. Shilova, I. I. Mikhalyov, I. M. Molotkovskaya, S. A. Akimov, and O. V. Batishchev, Line activity of ganglioside GM1 regulates the raft size distribution in a cholesterol-dependent manner, Langmuir **33**, 3517 (2017).

[16] G. Staneva, D. S. Osipenko, T. R. Galimzyanov, K. V. Pavlov, and S. A. Akimov, Metabolic precursor of cholesterol causes formation of chained aggregates of liquid-ordered domains, Langmuir **32**, 1591 (2016).

[17] W. J. Sun, S. Tristram-Nagle, R. M. Suter, and J. F. Nagle, Structure of gel phase saturated lecithin bilayers: Temperature and chain length dependence, Biophys. J. **71**, 885 (1996).

[18] K. Y. C. Lee, A. Gopal, A. von Nahmen, J. A. Zasadzinski, J. Majewski, G. S. Smith, P. B. Howes, and K. Kjaer, Influence of palmitic acid and hexadecanol on the phase transition temperature and molecular packing of dipalmitoylphosphatidyl-choline monolayers at the air–water interface, J. Chem. Phys. **116**, 774 (2001).

[19] G. Ma and H. C. Allen, DPPC Langmuir monolayer at the air–water interface: Probing the tail and head groups by vibrational sum frequency generation spectroscopy, Langmuir **22**, 5341 (2006).

[20] J. F. Nagle, Theory of lipid monolayer and bilayer phase transitions: Effect of headgroup interactions, J. Membr. Biol. **27**, 233 (1976).

[21] T. J. McIntosh, Differences in hydrocarbon chain tilt between hydrated phosphatidylethanolamine and phosphatidylcholine bilayers. A molecular packing model, Biophys. J. **29**, 237 (1980).

[22] S. A. Safran, M. O. Robbins, and S. Garoff, Tilt and splay of surfactants on surfaces, Phys. Rev. A **33**, 2186 (1986).

[23] S. Tristram-Nagle, R. Zhang, R. M. Suter, C. R. Worthington, W. J. Sun, and J. F. Nagle, Measurement of chain tilt angle in fully hydrated bilayers of gel phase lecithins, Biophys. J. **64**, 1097 (1993).

[24] B. Kheyfets, T. Galimzyanov, and S. Mukhin, Microscopic description of the thermodynamics of a lipid membrane at a liquid–gel phase transition, JETP Lett. **107**, 718 (2018).

[25] T. Baumgart and A. Offenhäusser, Lateral diffusion in substrate-supported lipid monolayers as a function of ambient relative humidity, Biophys. J. **83**, 1489 (2002).

[26] E. Sackmann, Supported membranes: Scientific and practical applications, Science **271**, 43 (1996).

[27] S. I. Mukhin and S. Baoukina, Analytical derivation of thermodynamic characteristics of lipid bilayer from a flexible string model, Phys. Rev. E **71**, 061918 (2005).

[28] S. I. Mukhin and B. B. Kheyfets, Analytical approach to thermodynamics of bolalipid membranes, Phys. Rev. E **82**, 051901 (2010).

[29] S. I. Mukhin and B. B. Kheyfets, Pore formation phase diagrams for lipid membranes, JETP Lett. **99**, 358 (2014).

[30] B. Kheyfets, T. Galimzyanov, A. Drozdova, and S. Mukhin, Analytical calculation of the lipid bilayer bending modulus, Phys. Rev. E **94**, 042415 (2016).

[31] B. Kheyfets, T. Galimzyanov, and S. Mukhin, Lipid lateral self-diffusion drop at liquid-gel phase transition, Phys. Rev. E **99**, 012414 (2019).

[32] T. W. Burkhardt, Free energy of a semiflexible polymer confined along an axis, J. Phys. A **28**, L629 (1995).

[33] I. Szleifer, D. Kramer, A. Ben-Shaul, D. Roux, and W. M. Gelbart, Curvature Elasticity of Pure and Mixed Surfactant Films, Phys. Rev. Lett. **60**, 1966 (1988).

[34] I. Szleifer, D. Kramer, A. Ben-Shaul, W. M. Gelbart, and S. A. Safran, Molecular theory of curvature elasticity in surfactant films, J. Chem. Phys. **92**, 6800 (1990).

[35] E. Lindahl and O. Edholm, Mesoscopic undulations and thickness fluctuations in lipid bilayers from molecular dynamics simulations, Biophys. J. **79**, 426 (2000).

[36] L. Vermeer, B. de Groot, V. e. Réat, A. Milon, and J. Czaplicki, Acyl chain order parameter profiles in phospholipid bilayers: Computation from molecular dynamics simulations and comparison with ^{2}H NMR experiments, Eur. Biophys. J. **36**, 919 (2007).

[37] D. Feng and G. Jin, *Introduction to Condensed Matter Physics* (World Scientific, Singapore, 2005).

[38] T. T. Mills, G. E. S. Toombes, S. Tristram-Nagle, D.-M. Smilgies, G. W. Feigenson, and J. F. Nagle, Order parameters and areas in fluid-phase oriented lipid membranes using wide angle X-ray scattering, Biophys. J. **95**, 669 (2008).

[39] J. N. Israelachvili, *Intermolecular and Surface Forces*, 3rd ed. (Academic Press, New York, 2011).

[40] S. Marčelja, Chain ordering in liquid crystals: II. Structure of bilayer membranes, Biochim. Biophys. Acta, Biomembr. **367**, 165 (1974).

[41] L. Salem, Attractive forces between long saturated chains at short distances, J. Chem. Phys. **37**, 2100 (1962).

[42] F. E. E. Harb, A. Simon, and B. Tinland, Ripple formation in unilamellar-supported lipid bilayer revealed by FRAPP, Eur. Phys. J. E **36**, 140 (2013).

[43] K. Akabori and J. F. Nagle, Structure of the DMPC lipid bilayer ripple phase, Soft matter **11**, 918 (2015).

[44] A. H. D. Vries, S. Yefimov, A. E. Mark, and S. J. Marrink, Molecular structure of the lecithin ripple phase, Proc. Nat. Acad. Sci. USA **102**, 5392 (2005).

[45] E. Maltseva and G. Brezesinski, Adsorption of amyloid beta (1-40) peptide to phosphatidylethanolamine monolayers, Chem. Phys. Chem. **5**, 1185 (2004).

[46] U. Bernchou, J. Brewer, H. S. Midtiby, J. H. Ipsen, L. A. Bagatolli, and A. C. Simonsen, Texture of lipid bilayer domains, J. Am. Chem. Soc. **131**, 14130 (2009).